Author: Please verify mean ± SD as added. Nonstandard abbreviations are written out, per journal style.

Quantitative Evaluation of Sonophoresis Efficiency and Its Dependence on Sonication Parameters and Particle Size

Kun Loong Lee, BS, Yufeng Zhou, PhD

Transdermal drug delivery makes a critical contribution to medical practice and some advantages over conventional oral administration and hypodermic injection. Enhancement of percutaneous absorption or penetration of therapeutic agents (ie, drugs and macromolecules) by ultrasound, termed *sonophoresis*, has been applied and studied for decades. In this study, the penetration percentage through porcine ear skin specimens was determined quantitatively by measuring the fluorescence from nanoparticles of 60, 220, and 840 nm in size in a receptor chamber at different sonication parameters (ie, duty cycle, 20%–100%; acoustic intensity, 0.3–1.0 W/cm^2; duration, 7–30 minutes; and frequency, 1 MHz). In general, the sonophoresis efficiency increased with the acoustic intensity, duty cycle, and sonication duration but decreased with the particle size (**mean ± SD**, 62.6% ± 5.4% for 60-nm versus 11.9% ± 1.1% for 840-nm polystyrene nanospheres after 30 minutes of sonication at 0.5 W/cm^2 and a 100% duty cycle; $P < .05$). On scanning electron microscopy the pore size remained the same (≈100 μm), but more flakes were observed with the progress of sonication. In summary, sonophoresis efficiency is dependent on the ultrasound parameters and particle size. Sufficient sonication would lead to satisfactory penetration of even submicrometer objects through the pores.

Key Words—cavitation damage; fluorescent nanoparticles; quantitative drug penetration percentage; sonophoresis; superficial structures; transdermal drug delivery

Received January 14, 2014, from the Division of Engineering Mechanics, School of Mechanical and Aerospace Engineering, Nanyang Technological University, Singapore (K.L.L., Y.Z.); and Key Laboratory of Modern Acoustics, Nanjing University, Nanjing, China (Y.Z.). Revision requested March 26, 2014. Revised manuscript accepted for publication June 26, 2014.

We thank Suresh Kanna Murugappan for help with scanning electron microscopy and conducting the experiments.

Address correspondence to Yufeng Zhou, PhD, School of Mechanical and Aerospace Engineering, Nanyang Technological University, 50 Nanyang Ave, Singapore, 639798.

E-mail: yfzhou@ntu.edu.sg

Abbreviations

PBS, phosphate-buffered saline; SEM, scanning electron microscopy

doi:10.7863/ultra.34.3.519

Oral administration and hypodermic injection are routine approaches for drug delivery to the circulation. However, they are associated with some shortcomings, such as premature drug metabolization by the first-pass effect of the liver and gut wall, degradation of drugs by the digestive tract, unstable plasma levels, difficulty of immediate termination, pain, dangerous medical waste, and risk of disease transmission by needle reuse.[1] Transporting therapeutic agents through the wide epidermis, known as transdermal drug delivery, is an attractive alternative to conventional approaches. Transdermal drug delivery is noninvasive in nature, and the systems can be self-administered, released over a long period, and inexpensive. Three generations of development have been undergone in **transdermal drug delivery**, such as chemical enhancers,[2] iontophoresis,[3] biochemical enhancers,[4] electroporation,[5] and microneedles.[6] These techniques are mostly reversible except microneedles. The skin structure and elasticity can be altered to enable increased permeation of compounds temporarily and resumed a few hours after termination without permanent damage.

However, only a limited number of drugs with molecular weights up to only a few hundred daltons, such as estradiol, fentanyl, lidocaine, and testosterone, are amenable to administration by the transdermal route for treatment of local allergies and infections. Delivery of peptides, hydrophilic drugs, and macromolecules (ie, DNA and small interfering RNA in genetic therapy) is still challenging for transdermal drug delivery. Therefore, although transdermal drug delivery has made a substantial contribution to medical practice, it only occupies about 10% of the entire drug delivery market.[7]

Ultrasound has been used in transdermal drug delivery since the 1950s in sports medicine as physical therapy, which is termed *sonophoresis* or *phonophoresis*.[8,9] Ultrasound can disrupt the lipid structure in the stratum corneum and thereby increase permeability by using either noncavitation or cavitation effects. Numerous studies have illustrated that sonophoresis is generally safe with no negative short- or long-term side effects. Noncavitation ultrasound is generally limited to enhancing small lipophilic compounds in transdermal drug delivery. In comparison, localized shock waves and high-speed liquid microjets directed at the stratum corneum could be produced as a result of bubble cavitation at the skin surface, which increases skin permeability for up to many hours without damaging deeper tissues. Tissue heating by absorbing acoustic energy is not a big concern at the energy level currently used. Sonophoresis has been approved by the US Food and Drug Administration for lidocaine and has been studied extensively for insulin, heparin, and the tetanus toxoid vaccine.[1,10]

To obtain maximum therapeutic efficacy, several new drug carriers have been investigated. Liposomes are biocompatible and biodegradable vesicles made of natural lipids with diameters of about 25 to 10,000 nm. Hydrophilic and lipophilic drugs can be encapsulated in the lipid walls and the aqueous interior of the liposomes, respectively. Transdermal delivery by liposomes is an interdisciplinary topic of great interest today.[11] Ethosomes are noninvasive delivery carriers that enable drugs to reach the deep skin layers or the systemic circulation.[12] If methotrexate, which is an antipsoriatic, antineoplastic, highly hydrosoluble agent with limited transdermal permeation, is loaded with ethosomal carriers in the optimal size of 143 ± 16 nm, an enhanced transdermal flux of 57.2 ± 4.34 μg/cm^2/h and a decreased lag time of 0.9 hours across human cadaver skin can be obtained.[13] Microparticles and nanoparticles consisting of proteins or biodegradable and biocompatible polymers, such as polylactide and poly(lactic-co-glycolic) acid, can incorporate drugs or antigens in the form of solid solutions or dispersions and have been shown to enhance the delivery of certain drugs across a number of natural and artificial membranes. Metal nanoparticles are recognized as having seemingly small druglike characteristics: ie, antimicrobial activity and skin cancer prevention. However, nanoparticles larger than 10 nm in diameter are unlikely to penetrate through the stratum corneum into viable human skin but will accumulate in the hair follicle openings, especially after massage.[14] Biodegradable nanoparticles (150–250 nm) have been used for transdermal DNA delivery into mouse skin using a low-pressure gene gun for enhanced gene expression.[15]

Sonication conditions are described by the frequency, acoustic intensity, duty cycle, and exposure duration. Although many investigations have demonstrated the effectiveness of sonophoresis both in vitro and in vivo, effects of ultrasound parameters on the outcome are not clear. Few studies have been done on the effects of sonophoresis on the penetration of large drug carriers. In this study, drug penetration efficiency was quantified by measuring the fluorescence of nanoparticles in a receptor chamber. The outcomes in porcine ear skin specimens of varying acoustic intensities (0.3–1.0 W/cm^2), duty cycles (20%–100%), and durations (7–30 minutes) for different polystyrene nanospheres (60, 220, and 840 nm) were studied. Sonicated samples were observed on scanning electron microscopy (SEM) for cavitation-induced damage. It was found that, owing to hair removal, sonophoresis had much higher penetration efficiency, even for submicrometer particles, which increased with the acoustic intensity, duty cycle, and sonication duration but decreased with the particle size.

Materials and Methods

Sample Preparation and Experimental Setup

Porcine ear skin was used in this study because of its similar dermatopharmacokinetic characteristics (ie, diffusion and partition of drugs in the stratum corneum) as human skin and was prepared by following previously described protocols.[16,17] Fresh porcine ears were purchased from a local slaughterhouse (Primary Industrial Pte, Ltd, Singapore) after approval from the Agri-Food Veterinary Authority of Singapore, cleaned under cold running water, and immersed in a phosphate-buffered saline (PBS) solution for 1 hour to remove remaining lipids or oil. Any visible hairs were carefully plucked out. Skin membranes were removed from the underlying cartilage within 24 hours of animal death, cut into the size of 2.3 × 2.3 cm, wrapped in aluminum foil, and then stored at –20°C for use within 3 months. About 3 samples were prepared from each ear. No notable differ-

ences in experimental results were found during the 3-month study. The thickness of the skin specimens was 1.5 ± 0.4 mm as measured by digital calipers (Wiha Digi-Max; Werkzeuge GmbH, Schonach, Germany). On the day of the experiment, the tissue samples were soaked in PBS at room temperature (23°C ± 1°C) for about 1 hour to thaw the specimens and to allow their initial barrier property to reach a steady state.

The skin membranes were mounted with the stratum corneum toward the ultrasound transducer. Sky blue–dyed polystyrene nanoparticles in sizes of 60, 220, and 840 nm (Spherotech, Lake Forest, IL) were used in this study because their emission and excitation wavelengths matched the fluorescent detector module. A 30-μL volume of nanoparticles was spread evenly across the specimen. Then an ultrasound transducer (Therasound Evo; Rich-Mar, Chattanooga, TN) with a driving frequency of 1 MHz, spatial-average temporal-peak intensity up to 2 W/cm^2 as calibrated by the manufacturer, varied duty cycles from 20% to 100% (continuous wave), and a diameter of 2 cm, which was aligned vertically by a chemical clap, was applied to the specimen. Similar transducers have been used widely in bioacoustic studies, such as sonoporation, sonothrombolysis, hyperthermia, and drug delivery to solid tumors and cancer in vivo. Before each experiment, the transducer was cleaned with distilled water 3 times to eliminate remaining particles. A receptor chamber filled with 2.6 mL of distilled water was placed underneath the skin sample and on the top of a piece of a rubber sheet with a thickness of about 5 mm to reduce the propensity of generating standing waves. The experimental setup is shown in Figure 1. The sonication time was set and controlled by the ultrasound apparatus, and the experimental conditions were randomly selected.

Fluorescence Detection and Nanoparticle Concentration Calibration

After the sonication, the solution in the receptor was mixed homogeneously, and then 1.3 mL of the solution was extracted to measure its fluorescent standard unit by a fluorometer (GloMax-Multi Jr; Promega, Madison, WI) using a green fluorescence optical kit with an excitation wavelength of 525 nm and an emission wavelength of 580 to 640 nm. Fluorescence standard units for varied concentrations of nanoparticles in the distilled water (30 μL in 2.6 mL of distilled water as 100%) were measured to draw a calibration curve, from which the concentration of nanoparticles in the receptor chamber and the corresponding penetration efficiency could be determined quantitatively.

Scanning Electron Microscopy

After the experiment, the skin specimen was washed with the PBS solution 3 times and fixed by 2.5% glutaraldehyde (Sigma-Aldrich, St Louis, MO) overnight at 4°C. Samples were washed the next day with PBS to remove glutaraldehyde, dehydrated with increasing concentrations of ethanol from 25% to 100%, dried using a critical point dryer (CPD 030; Bal-Tec, Witten, Germany), and then photographed by an SEM (JSM-5600LV; JEOL, Tokyo, Japan) with an appropriate magnification at different positions on the sonicated region to observe the morphologic changes.

Statistical Analysis

A 2-way analysis of variance (2-factor without replication; $P = .05$) was performed to test the statistical significance between the treatment protocols using SPSS software (IBM Corporation, Armonk, NY). The sample size in each test condition was at least 5, and all samples were completely independent.

Figure 1. Experimental setup for using ultrasound in transdermal drug delivery.

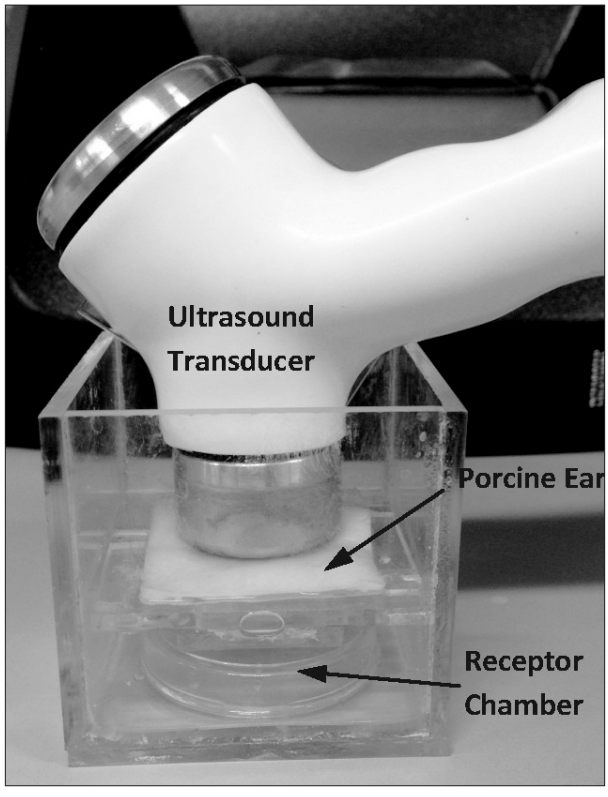

Author: Please verify mean ± SD as added. Also verify D as written out. In Table 1, please verify mean ± SD footnote as added

Results

Calibration

Fluorescent standard units for varied nanoparticle concentrations, from 10% to 100%, can be fit quite well by a straight line with zero bias as the error of the fluorescence detector (Figure 2). The variation is usually less than 0.3% except at the concentration of 100%, which may be due to interferences among concentrated nanoparticles. Such a variation becomes serious with a greater nanoparticle volume. Sonication at the intensity of 1.0 W/cm^2 and duty cycle of 100% or immersion in a water bath at temperatures of 24°C, 35°C, and 40°C for 30 minutes will not change the calibration results substantially (data not shown), which suggests stable fluorescence in cavitation and hyperthermia.

Penetration Efficiency

The penetration percentages of 220-nm nanoparticles after a 7-minute sonication at varied acoustic intensities and duty cycles are listed in Table 1. It was found that with the increase in acoustic intensity from 0.3 to 1.0 W/cm^2 and duty cycle from 20% to 100%, the drug penetration efficiency increased from a **mean ± SD** of 2.7% ± 0.7% to 10.2% ± 1.9%. The results for 60-, 220-, and 840-nm nanoparticles after 7-, 15-, and 30-minute sonications at the acoustic intensity of 0.5 W/cm^2 and duty cycle of 100% are shown in Figure 3. The dependencies on the particle size and sonication duration are apparent. For 60-nm nanoparticles, the transdermal penetration efficiency increased from 28.0% ± 2.3% at the 7-minute sonication to 62.6% ± 5.4% at the 30-minute sonication. For even submicrometer particles (840 nm, whose molecular weight is ≈1.69 ± 1011 Da),[18] satisfactory results could also be obtained after the 30-minute sonication (11.9% ± 1.1%). In addition, the temperature elevations in all conditions were less than 2°C as measured by a thermocouple (**diameter**, 0.5 mm) attached to the skin specimen and a thermometer (Omega, Stamford, CT) during the experiment, which were similar to the findings for sonication by 10 MHz over 2 hours.[19] Therefore, a thermal effect is not the major mechanism for the enhanced penetration. With consideration of the heat sink effect, its contribution will be even lower in vivo.

Scanning Electron Microscopy

Scanning electron microscopic images of specimens after the 7-minute sonication at the acoustic intensity of 0.5 W/cm^2 and duty cycles of 20%, 50%, and 100% did not show permanent or substantial damage on the skin, but a little flaking occurred inside and around the skin pore at the 100% duty cycle (data not shown). Such an observation became more notable with increases in the sonication duration (Figure 4). Stratum corneum surfaces within the pore

Table 1. Penetration of 220-nm Nanoparticles After 7-Minute Sonication at Various Duty Cycles and Acoustic Intensities

	Nanoparticle Penetration, %		
Duty Cycle, %	0.3 W/cm^2	0.5 W/cm^2	1.0 W/cm^2
20	2.7 ± 0.7	2.9 ± 0.6	3.5 ± 0.8
50	4.0 ± 1.1	4.4 ± 1.0	6.1 ± 1.3
100	5.4 ± 1.4	8.1 ± 1.6	10.2 ± 1.9

Data are presented as mean ± SD.

Figure 2. Relationship between fluorescence standard units and 220-nm fluorescent nanoparticle concentrations.

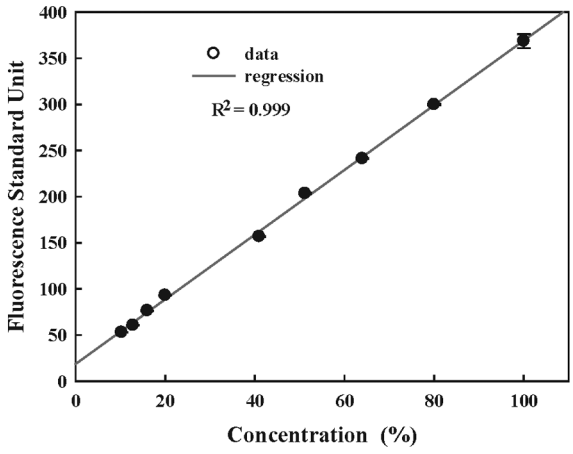

Figure 3. Transdermal drug penetration efficiencies using ultrasound at the acoustic intensity of 0.5 W/cm^2 for 60-, 220-, and 840-nm fluorescent nanoparticles after sonication for 7, 15, and 30 minutes.

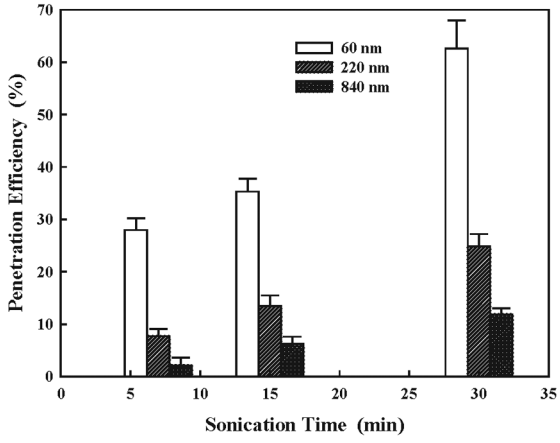

of untreated skin were arranged in an orderly and intact manner with parallel contours. Surfaces surrounding the pore were covered by overlapping corneocytes (Figure 4a). After the 7-minute sonication, an uneven surface emerged, and flakes started to appear (Figure 4b). Although the clearing of keratinocytes was slight, the flakes were still firmly attached to the skin. The appearance of such flakes may have been due to stress induced by the bubble cavitation in the acoustic field. The disruption of the corneocytes and keratinocytes was more profound for the 15- and 30-minute sonications (Figure 4, c and d). The corneocytes were disintegrated, with flakes of detached keratinocytes spreading across the surface. Similar damage patterns but less severity were also found in the spaces between pores. In addition, regardless of the sonication duration, the pore sizes were almost unchanged (≈100 μm). No other damage, either skin burns or large mechanical holes, was found on SEM.

Discussion

Initially, ultrasound-induced convection was not considered a driving force in drug transport because no differences in mannitol for porcine skin penetration were observed with and without sonication.[20] Usually a skin specimen was sonicated for a certain time, and then the drug was spattered for passive penetration. However, the difference became significant for larger molecules, such as insulin.[21] When the acoustic wave propagates through a medium, scattering will occur at a particle if its size is much smaller than the wavelength (ie, 1.5 mm at 1 MHz). Attenuation, including both scattering and absorption, of the acoustic wave leads to energy deposition. The transferred momentum in the direction of wave propagation generates a force that results in displacement of the particle. The acoustic radiation force dominates for a large product of the wave-

Figure 4. Representative SEM images photos of porcine skin samples (**a**) and tissue samples after sonication of for 7 (**b**), 15 (**c**), and 30 (**d**) minutes at the acoustic intensity of 0.5 W/cm^2 with a 100% duty cycle (continuous wave).

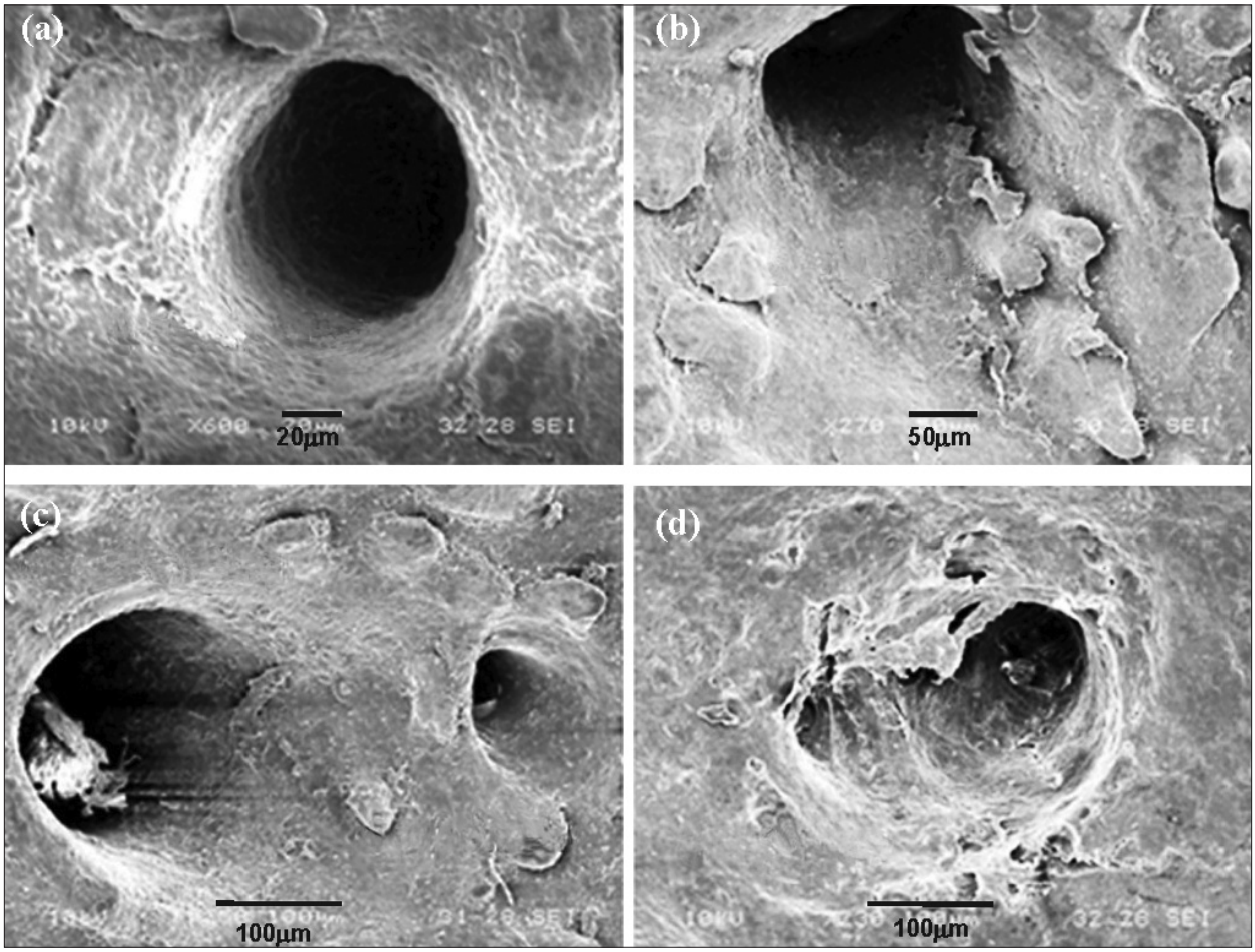

Author: Please verify kDa as added.

length and particle radius (the scattering cross section is proportional to k^4a^6, where k is the wave number, and a is the sphere radius) and may explain the outcome discrepancy in sonophoresis.[22] Use of the acoustic radiation force could also enhance the activation of nanoparticles in cancer cells.[23]

Bubble cavitation is believed to be one of the major mechanisms in sonophoresis, leading to increased permeability. Sonication at 168 kHz with a spatial-average pressure amplitude of 190 kPa could generate defects (entrapped air pockets with a size of 20 μm) in the stratum corneum to allow the transdermal passage of high-molecular-weight drugs.[24] Cavitation could also occur in vivo in 5-μm sweat and sebaceous gland ducts with no histologic changes.[25] The cavitation threshold in liquids depends on both environmental properties (ie, pressure, temperature, viscosity, and gas concentration) and ultrasound parameters (ie, frequency, pulse duration, and duty cycle), and the measured value is determined by the sensitivity of the detection system and method.[26] Therefore, there are variations in the reported thresholds in water at 1 MHz: ie, approximately 118 kPa,[27] 0.46 ± 0.21 MPa,[26] approximately 0.23 MPa,[28] approximately 0.69 MPa,[29] approximately 0.47 MPa,[30] and approximately 0.23 MPa.[31] The Blake threshold for cavitation inception in water varies theoretically from 0.15 to 0.6 MPa for initial bubble radii of 1.0 to 0.1 μm, respectively.[26] In addition, the cavitation threshold decreases with the pulse duration and pulse repetition frequency, the progress of sonication, and the presence of nanoparticles.[32] Therefore, the acoustic intensity of 0.5 W/cm^2 used in this study (122 kPa) may induce bubble cavitation at a certain temporal point during a long sonication in the polystyrene nanosphere solution. The presence of crevices in solids (or pores in the skin) can attract bubbles for stronger cavitation due to surface tension.[33,34] In comparison, confocal microscopy indicates a structure disorder in the lipid bilayers of the stratum corneum induced by cavitation in the keratinocytes on ultrasound exposure (frequency of 1–3 MHz and intensity of 0–2 W/cm^2), thereby enhancing transdermal transport. More cavitation at the skin surface may explain the discrepancy between results in this study and the reported ones.

A theoretical model predicts that sonophoretic enhancement depends mostly on passive permeant diffusion by sonication, rather than on permeation through the skin, which agrees quantitatively with the experimental results of a variety of permeants.[35] Meanwhile, a high-speed jet impact at the collapse stage of a cavitation bubble can also pump the liquid through a hole, and the pumping effect is fairly robust for different alignments.[36,37] If the ratio of the hole diameter to the maximum bubble size is large (as the pore in our skin sample), the jet impact occurs away from the boundary, and the bubble moves into the hole at a very high speed (≈24 m/s) with a considerable amount of fluid. If the distance between the cavitation site and the hole is less than the maximum bubble radius, the bubble will enter the hole during its expansion phase, and a toroidal cavitation bubble will form near the edge of the hole, whose collapse may be the reason for the damage surrounding the pore entry on our SEM images. Further work is required to investigate the bubbles induced by sonication, their location around the pore, and the pumping effect of particle transport, which may enhance our understanding of the role of bubble cavitation in sonophoresis and subsequently improve its efficiency. Overall, cavitation on the surface of and within the skin and associated microstreaming may work synergistically to enhance pharmacokinetics.

The other mechanism is the thermal effect. Although the acoustic absorption of tissue is substantial at high frequencies, the temperature elevation in the porcine ear skin over a 2-hour sonication at 10 MHz was negligible (<2°C). In contrast, the corresponding average temperature increase produced by 20 kHz at the intensity of 15 W/cm^2 was 20°C. The bubbles induced by acoustic waves can enhance the energy deposition and temperature elevation in ultrasound hyperthermia.[38] Therefore, the temperature rise is not a major mechanism at high frequencies to promote drug transport, but it is at low frequencies.

High-frequency ultrasound has been shown to be effective for low-molecular-weight drugs (<500 Da) across human skin, whereas low-frequency ultrasound is up to 3 orders of magnitude more effective at increasing skin penetration, such as for interferon-γ (17 kDa) and erythropoietin 48 (kDa).[8] The molecular weights of the 60-, 220-, and 840-nm polystyrene nanospheres used in our experiment are 7.15×10^7, 3.53×10^9, and 1.69×10^{11} **kDa**, respectively.[18] The discrepancy may have been due to the preexisting pores in the porcine ear skin specimens (≈100 μm, which were much larger than the holes produced by bubble cavitation [1–3 μm[39]] and sweat pores [≈20 nm]), long continuous sonication, and less interaction of the polystyrene materials with the biological tissue. Hair removal (ie, using cream), which could enhance the efficiency of transdermal drug delivery substantially, as shown in this study, is not prohibited in clinics. Transdermal delivery of macromolecules and vaccines is of great interest and potential, with continuous investigation. The sophistication of devices for effective sonication is considered a hindrance for wide application.[1] Recently, a

wearable battery-operated therapeutic ultrasound device with the capability of self-operation for up to 6 hours daily was designed and evaluated in patients with chronic trapezius myofascial pain.[40] The intensity is 0.03 to 2.0 W/cm^2, and the size of the radiofrequency driver is only 15 × 18 mm. This device makes long sonication during sonophoresis for clinical use possible, instead of only a few seconds before drug use.

Partial-thickness samples, including tissue culture–derived skin equivalents (ie, living skin–equivalent models) and a human reconstructed epidermis, have also been used as alternatives to animal skins in transdermal delivery studies.[41] Living skin–equivalent models have a dermis, an epidermis, and a partially differentiated stratum corneum, but are deficient in skin appendages (ie, pilosebaceous units, hair follicles, and sweat glands). As a result, an 800- to 900-fold higher flux was achieved by using living skin–equivalent models than full-thickness human skin because of the differences in structures and lipid compositions.[42] The permeability coefficient for cadaver skin increased with the carbon chain length, which was not observed with the use of living skin–equivalent models.[43] Therefore, skin cultures are not recommended in skin permeation studies because of their much lower barrier properties, cost, and data reproducibility. In comparison, porcine skin was found to have closer permeability characteristics than rat skin to human skin, particularly for lipophilic penetrants, which may be attributed to similar surface lipids, barrier thicknesses (21–26 μm for the stratum corneum and 66–72 μm for the epidermis in porcine ear skin versus 10–40 μm for the stratum corneum in the human abdomen and 70 μm for the epidermis in the human shoulder) and morphologic aspects (ie, 20 hairs per 1 cm^2 in porcine ear skin are comparable to 14–24 in human skin).[44] Furthermore, another limitation of in vitro studies is the absence of muscle and circulating blood in the tested specimen. Therefore, the drug absorption and the subsequent outcome cannot be evaluated, which needs to be done in live animals.

References

1. Prausnitz MR, Langer R. Transdermal drug delivery. *Nat Biotechnol* 2008; 26:1261–1268.
2. Barry BW. Mode of action of penetration enhancers in human skin. *J Control Release* 1987; 6:85–97.
3. Prausnitz MR, Bose VG, Langer R, Weaver JC. Electroporation of mammalian skin: a mechanism to enhance transdermal drug delivery. *Proc Natl Acad Sci USA* 1993; 90:10504–10508.
4. Williams AC, Barry BW. Penetration enhancers. *Adv Drug Deliv Rev* 2004; 56:603–618.
5. Denet AR, Vanbever R, Preat V. Skin electroporation for transdermal and topical delivery. *Adv Drug Deliv Rev* 2004; 56:659–674.
6. Sivamani RK, Liepmann D, Maibach HI. Microneedles and transdermal applications. *Expert Opin Drug Deliv* 2007; 4:19–25.
7. Brown BAS. Five myths about MDIs. *Drug Deliv Technol* 2002; 3:1–11.
8. Mitragotri S, Blankschtein D, Langer R. Ultrasound-mediated transdermal protein delivery. *Science* 1995; 269:850–853.
9. Byl NN. The use of ultrasound as an enhancer for transcutaneous drug delivery: phonophoresis. *Phys Ther* 1995; 75:539–553.
10. Polat BE, Hart D, Langer R, Blankschtein D. Ultrasound-mediated transdermal drug delivery: mechanism, scope, and emerging trends. *J Control Release* 2011; 152:330–348.
11. Touitou E, Junginger HE, Weiner ND, Nagai T, Mezei M. Liposomes as carriers for topical and transdermal delivery. *J Pharm Sci* 1994; 83:1189–1203.
12. Godin B, Touitou E. Ethosomes: new prospects in transdermal delivery. *Crit Rev Ther Drug Carrier Syst* 2003; 20:63–102.
13. Dubey V, Mishra D, Dutta T, Nahar M, Saraf DK, Jain NK. Dermal and transdermal delivery of an anti-psoriatic agent via ethanolic liposomes. *J Control Release* 2007; 123:148–154.
14. Prow TW, Grice JE, Lin LL, et al. Nanoparticles and microparticles for skin drug delivery. *Adv Drug Deliv Rev* 2011; 63:470–491.
15. Lee PW, Peng SF, Su CJ, et al. The use of biodegradable polymeric nanoparticles in combination with a low-pressure gene gun for transdermal DNA delivery. *Biomaterials* 2008; 29:742–751.
16. Herkenne C, Naik A, Kalia YN, Hadgraft J, Guy RH. Pig ear skin ex vivo as a model for in vivo dermatopharmacokinetic studies in man. *Pharm Res* 2006; 23:1850–1856.
17. Sekkat N, Kalia YN, Guy RH. Biophysical study of porcine ear skin in vitro and its comparison to human skin in vivo. *J Pharm Sci* 2002; 91:2376–2381.
18. Peng WP, Yang YC, Lin CW, Chang HC. Molar mass and molar mass distribution of polystyrene particle size standard. *Anal Chem* 2005; 77:7084–7089.
19. Merino G, Kalia YN, Delgado-Charro MB, Potts RO, Guy RH. Frequency and thermal effects on the enhancement of transdermal transport by sonophoresis. *J Control Release* 2003; 88:85–94.
20. Mitragotri S, Farell J, Tang H, Terahara T, Kost J, Langer R. Determination of threshold energy dose for ultrasound-induced transdermal transport. *J Control Release* 2000; 63:41–52.
21. Boucaud A, Garrigue MA, Machet L, Vaillant L, Patat F. Effect of sonication parameters on transdermal delivery of insulin to hairless rats. *J Control Release* 2002; 81:113–119.
22. King LV. On the acoustic radiation pressure on spheres. *Proc R Soc Lond A* 1934; 147:212–240.
23. Crowder KC, Hughes MS, Marsh JN, et al. Sonic activation of molecularly-targeted nanoparticles accelerates transmembrane lipid delivery to cancer cells through contact-mediated mechanisms: implications for enhanced local drug delivery. *Ultrasound Med Biol* 2005; 31:1693–1700.
24. Wu J, Chappelow J, Yang J, Weimann L. Defects generated in human stratum corneum specimens by ultrasound. *Ultrasound Med Biol* 1998; 24:705–710.

Author: Please give page numbers for reference 31.

25. Machet L, Boucaud L. Phonophoresis: efficiency, mechanisms and skin tolerance. *Int J Pharm* 2002; 243:1–15.
26. Fowlkes JB, Crum LA. Cavitation threshold measurements for microsecond length pulses of ultrasound. *J Acoust Soc Am* 1988; 83:2190–2201.
27. Sponer J. Dependence of the cavitation threshold on the ultrasonic frequency. *Czech J Phys* 1990; 40:1123–1132.
28. Connolly W, Fox FE. Ultrasonic cavitation thresholds in water. *J Acoust Soc Am* 1954; 26:843–848.
29. Coakley WT. Acoustic detection of single cavitation events in a focused field in water at 1 MHz. *J Acoust Soc Am* 1971; 49:792–801.
30. Ciaravino V, Miller MW. A comparison of two techniques for measured iodine release as an indicator of acoustic cavitation. *J Acoust Soc Am* 1983; 74:1813–1816.
31. Vaughan PW, Leeman S, Hedges M, Graham E, Suton P. Cavitation effects at megahertz frequencies. In: Lauterborn W (ed). *Cavitation and Inhomogeneities in Underwater Acoustics*. Berlin, Germany: Springer; 1980.
32. Smith MJ, Ho VHB, Darton NJ, Slater NKH. Effect of magnetite nanoparticle agglomerates on ultrasound induced inertial cavitation. *Ultrasound Med Biol* 2009; 35:1010–1014.
33. Pishchalnikov YA, Sapozhnikov OA, Bailey MR, et al. Cavitation bubble cluster activity in the breakage of kidney stone by lithotripter shockwaves. *J Endourol* 2003; 17:435–447.
34. Leighton TG. Bubble populaiton phenomena in acoustic cavitation. *Ultrason Sonochem* 1995; 2:S123–S126.
35. Mitragotri S, Edwards DA, Blankschtein D, Langer R. A mechanistic study of ultrasonically-enhanced transdermal drug delivery. *J Pharm Sci* 1995; 84:697–706.
36. Lew SFK, Klaseboer E, Khoo BC. A collapsing bubble-induced micropump: an experimental study. *Sensors Actuators A Phys* 2007; 133:161–172.
37. Khoo BC, Klaseboer E, Hung KC. A collapsing bubble-induced micropump using the jetting effect. *Sensors Actuators A Phys* 2005; 118:152–161.
38. Fujishiro S, Mitsumori M, Nishimura Y, et al. Increased heating efficiency of hyperthermia using an ultrasound contrast agent: a phantom study. *Int J Hyperthermia* 1998; 14:495–502.
39. Machet L, Cochelin N, Patat F, et al. In vitro phonophoresis of mannitol, oestradiol and hydrocortisone across human and hairless mouse skin. *Int J Pharm* 1998; 165:169–174.
40. Lewis GKJ, Langer MD, Henderson CRJ, Ortiz R. Design and evaluation of a wearable self-applied therapeutic ultrasound device for chronic myofascial pain. *Ultrasound Med Biol* 2013; 39:1429–1439.
41. Argemi A, Domingo C, de Sousa AR, Duarte CM, Garcia-González CA, Saurina J. Characterization of new topical ketoprofen formulations prepared by drug entrapment in solid lipid matrices. *J Pharm Sci* 2011; 100:4783–4789.
42. Schmook FP, Meingassner JG, Billich A. Comparison of human skin or epidermis models with human and animal skin in in-vitro percutaneous absorption. *Int J Pharm* 2001; 14:51–56.
43. Roy SD, Fujiki J, Fleitman JS. Permeabilities of alkyl p-aminobenzoates through living skin equivalent and cadaver skin. *J Pharm Sci* 1993; 82: 1266–1268.
44. Godin B, Touitou E. Transdermal skin delivery: predictions for humans from in vivo, ex vivo and animal models. *Adv Drug Deliv Rev* 2007; 59:1152–1161.